Enhancement of Methanol Selectivity in the Products of Direct Selective Oxidation of Methane in CH_4–O_2–NO with Cu–ZnO/Al_2O_3

Tetsuya Takemoto,* Dehua He,† Yonghong Teng,* Akira Nakayama,* Kenji Tabata,*·‡·1 and Eiji Suzuki*·‡

*Catalysis Science Laboratory, Research Institute of Innovative Technology for the Earth (RITE), Kizugawadai, Kizu-cho, Soraku-gun, Kyoto 619-0292, Japan; †State Key Laboratory of C1 Chemical Technology, Department of Chemistry, Tsinghua University, Beijing 100084, China; and ‡Graduate School of Materials Science, Nara Institute of Science and Technology (NAIST), Takayama-cho, Ikoma, Nara 630-0101, Japan

Enhancement of methanol selectivity in the products of the direct selective oxidation of methane with CH_4–O_2–NO in a gas-phase reaction was examined using a Cu–ZnO/Al_2O_3 catalyst. Three distinct reaction paths over the Cu–ZnO/Al_2O_3 catalyst were detected in the gas-phase selective oxidation of methane in CH_4–O_2–NO. The formation of CH_3OH from CH_2O–H_2 and the water–gas shift reaction of CO–H_2O progressed chiefly at around 250°C over Cu–ZnO/Al_2O_3 catalyst. The steam reforming reaction of CH_3OH progressed over the same Cu–ZnO/Al_2O_3 catalyst at around 350°C and higher. Both CH_3OH and CH_2O were observed as C_1-oxygenates at 550°C in the gas-phase selective oxidation of methane in CH_4–O_2–NO, but only CH_3OH was observed as a C_1-oxygenate in the presence of Cu–ZnO/Al_2O_3 catalyst in addition to the gas-phase selective oxidation of methane. The complete exhaustion of oxygen in the gas-phase selective oxidation of methane in CH_4–O_2–NO was a key to the effective use of Cu–ZnO/Al_2O_3 catalyst. Of the two reactions, CH_3OH formation and water–gas shift over Cu–ZnO catalyst, the water–gas shift reaction progressed more over the catalyst with a higher surface area and with a lower surface Cu/Zn atomic ratio. © 2001 Academic Press

Key Words: selective oxidation; methane; methanol; NO$_x$; Cu–ZnO/Al_2O_3.

INTRODUCTION

Direct selective oxidation of methane to C_1-oxygenates (methanol and formaldehyde) with oxygen is a potentially important process not only for the effective use of natural gas resources but also for minimization of energy consumption. Various research studies on noncatalytic or catalytic oxidation of methane to oxygenates have been carried out since the early 1900s, but the main products were still carbon oxides (1–4). The rate-determining step in the direct selective oxidation of methane is the first hydrogen abstraction from methane. Therefore much research using initiators or sensitizers has been carried out to reduce the activa-

tion energy of the first hydrogen abstraction from methane. NO$_x$ ($x = 1$, 2) has been reported to be an effective initiator for the activation of methane (5–9). Very recently, Teng *et al.* (10) and Tabata *et al.* (11) systematically examined the effects of variation of reaction conditions on the yield of C_1-oxygenates in the gas-phase selective oxidation of methane in CH_4–O_2–NO$_x$ ($x = 1$, 2). The selectivity of both methanol and formaldehyde depended strongly on the reaction conditions, i.e., NO$_x$ concentration, CH_4/O_2 ratio, and space velocity (SV); however, these two products were always observed more or less in the reactions examined. It is important to control the selectivities of methanol and formaldehyde in the products for application as a practical process in the gas-phase selective oxidation of methane. We examined enhancement of the selectivity of methanol, which is a more admirable product in the selective oxidation of methane. Cu–ZnO-based catalyst is well known catalyst its high performance not only in a water–gas shift reaction (12) but also in a methanol synthesis reaction from CO/H_2 (13, 14). We attempt to examine the enhancement of selectivity of methanol in the gas-phase direct selective oxidation of methane using Cu–ZnO supported on Al_2O_3 catalyst through the catalytic hydrogenation of products in the gas-phase selective oxidation of methane in CH_4–O_2–NO. It is expected that hydrogen will be produced through the water–gas shift reaction (WGSR) between CO and H_2O. The WGSR could progress over Cu–ZnO/Al_2O_3 under a reduction conditions. No research has been reported on the application of the WGSR so as to enhance the selectivity of methanol in the direct selective oxidation of methane as far as we know. We examine the catalytic performance of Cu–ZnO/Al_2O_3 catalyst in the selective oxidation of methane so as to enhance the selectivity of methanol in the products.

EXPERIMENTAL

CH_4–O_2–NO reaction. Highly purified methane (>99.9995%), oxygen (>99.9999%), and 3.0% NO (Ar balance) were mixed with argon (>99.9999%). The

standard feed gas composition (77.5% CH_4, 5.8% O_2, 0.5% NO, Ar balance) was controlled with a mass flow controller except in the test on the effects of the CH_4/O_2 ratio. A quartz tube (7-mm i.d.) was mounted inside a stainless-steel tube (13.8-mm o.d.) to minimize the effects of the reactor wall. This quartz tube was heated for the gas-phase selective oxidation of methane with an electric furnace from the outside of the stainless-steel tube; the length of the heated zone was 100 mm. The temperature of the gas-phase reaction was measured at the center part of the electric furnace with a thermocouple, which was mounted in the center of the reactor. The thermocouple was covered with a quartz tube (3-mm o.d.) to avoid any reactions on the surface of the thermocouple. Two types of commercial Cu–ZnO supported on Al_2O_3 catalyst were obtained from Catalysts and Chemicals Inc, Far East. The catalyst was mounted 150 mm downstream from the end of the heater. The temperature of the catalyst was measured from outside the reactor with a thermocouple. Since the temperature of the mounted catalyst was less than 150°C without heating during the gas-phase reaction at 550°C, we controlled the temperature of the catalyst at 250°C with the other heater. The length of this heater was 100 mm. We used mechanical seals to connect the quartz and stainless-steel tubes, avoiding direct contact between reaction gas and the stainless-steel tube. Except for the tests on the effects of SV, the reaction gas was stabilized at 120 ml min^{-1} (SV = 15,700 h^{-1}) in every test. SV was calculated by dividing the gas flow volume per 1 h at 25°C and atmospheric pressure by the volume of the catalyst (0.5 g). The reaction pressure was kept at 0.5 MPa. The mixed gas was fed from the bottom side of the reactor. Products were analyzed with two on-line gas chromatographs. Carbon monoxide, carbon dioxide, ethane, ethene, formaldehyde, methanol, and nitromethane were detected with a flame ionization detector (FID, Gaskuropack 54) using a methanizer. Methane and oxygen were detected with a thermal conductivity detector (TCD, activated carbon). The carbon balance between the reactants and the products exceeded 95%. Every feed gas was mixed just before the inlet of the reactor. All of the gas lines from the exit of the reactor up to the gas chromatograph were heated at 120°C to avoid condensation. All the experiments were repeated at least three times to check reproducibility. The deviation of experimentally obtained results was less than ±1%.

CH_2O–H_2 reaction. The same two types of Cu–ZnO/ Al_2O_3 commercial catalysts were pretreated in a hydrogen– argon stream (10% H_2, 100 ml/min) at 250°C for 3 h. Catalytic hydrogenation of formaldehyde with these catalysts was carried out at atmospheric pressure with a conventional fixed-bed continuous flow quartz tube reactor (10.5-mm i.d.). The temperature of Cu–ZnO/Al_2O_3 was measured in the center of the electric furnace with a thermocouple, which was mounted in the center of the catalyst. The thermocouple was covered with a quartz tube (3-mm o.d.). The

temperature of the catalyst was controlled with an electric furnace from outside the quartz tube; the length of the heated zone was 100 mm. Commercial formaldehyde solution (37.0 wt% formaldehyde, 7.0 wt% methanol; Sigma– Aldrich Japan K.K.) was used as the source of formaldehyde. Formaldehyde solution was supplied with a micro-high-performance liquid chromatography pump, and it was evaporated in an evaporator. Standard reaction conditions were as follows: catalyst weight, 1.00 g; feed gas composition, CH_2O 5.0%, H_2 38.6%, CH_3OH 0.9%, H_2O 12.7%, Ar balance; total flow rate, 70 ml/min. The products were analyzed with an on-line gas chromatograph with a FID (Gaskuropack-54). The conversion of formaldehyde was calculated on the basis of the amount of formaldehyde supplied. The selectivity of methanol was calculated as modified selectivity. The amount of methanol subtracted (i.e., the amount of methanol in the feed gas was subtracted from the amount of methanol produced) in the products was used as the amount of converted formaldehyde.

Water–gas shift reaction of CO. The water–gas shift reaction of CO was examined over Cu–ZnO/Al_2O_3 with the same reactor used in the reaction of CH_4–O_2–NO at 0.5 MPa. The catalyst was mounted at the center of the electric furnace. The sample weight was 0.5 g. The temperature of Cu–ZnO/Al_2O_3 was measured in the center of the electric furnace with a thermocouple, which was mounted in the center of the catalyst. The temperature of the catalyst was controlled with an electric furnace from outside the stainless-steel tube; the length of the heated zone was 100 mm. The feed gas composition was as follows: CO 6.4%, CO_2 8.2%, H_2O 42.6%, H_2 41.2%, CH_4 1.6%. H_2O was vaporized in front of the entrance to the reactor with an electric heater. The total flow rate was 10 ml/min. The temperature of the catalyst was 250°C. The products were analyzed with two on-line gas chromatographs. Carbon monoxide and carbon dioxide were detected with a FID (Gaskuropack 54) using a methanizer. Methane and hydrogen were detected with a TCD (activated carbon).

Simulation of thermodynamic equilibrium of products. The calculations of thermodynamic equilibrium were carried out with the CHEMKIN III program (15, 16) using the thermodynamic database of Kee *et al.* (17). The EQUIL software package was used as the application code of the calculations. Thermodynamic equilibrium was calculated under the same reaction conditions as in the experiment minimizing the free energy of the products.

Characterization of Cu–ZnO/Al_2O_3. The atomic ratio Cu : Zn : Al of the sample was measured with energy-dispersive X-ray spectroscopy (EDX, KEVEX-Sigma). BET specific surface area was determined by N_2 adsorption at 77 K. The XRD (powder X-ray diffraction) pattern was recorded with an X-ray diffractometer (RINT

2000, Rigaku) using Cu$K\alpha$ radiation. The surface of sample was examined by X-ray photoelectron spectroscopy (XPS, ESCA-3200, Shimadzu) with an Mg$K\alpha$ X-ray source operating at 8 kV and 20 mA. Cu $2p$, Zn $2p$, Al $2p$, O $1s$, and C $1s$ levels spectra were investigated and their binding energies were calibrated using the main peak of the C $1s$ level spectrum of contaminated carbon at 284.8 eV as an internal reference.

RESULTS

3.1. Characterization of Cu–ZnO/Al$_2$O$_3$

The Cu : Zn : Al atomic ratios of the two samples obtained were examined with EDX. The Cu : Zn : Al ratios for two samples were 39.7 : 40.8 : 19.5 (denoted sample A) and 23.7 : 41.3 : 35.0 (denoted sample B). The specific surface areas were 68.7 and 93.1 m^2/g, respectively. XRD patterns of these samples were almost identical, and several peaks assignable to ZnO and CuO and confused other peaks were observed in the spectra of the untreated samples. These XRD patterns showed the samples were mixed states. The surface Cu/Zn atomic ratios were calculated from the proportion of each peak area of the Cu $2p$ level and the Zn $2p$ level spectra measured with XPS. With respect to each sensitivity factor, the set of elemental sensitivity factors of the equipment was used. The Cu–Zn ratios of samples A and B were 0.88 and 0.65, respectively.

Figure 1 shows the selectivities of products in methane selective oxidation in the absence of catalyst and in the presence of Cu–ZnO/Al$_2$O$_3$ catalyst. The selectivity of every product was measured after reaction for 180 min. The temperature of the gas-phase reaction and that of the catalyst were stabilized at 550 and 250°C, respectively. Methane
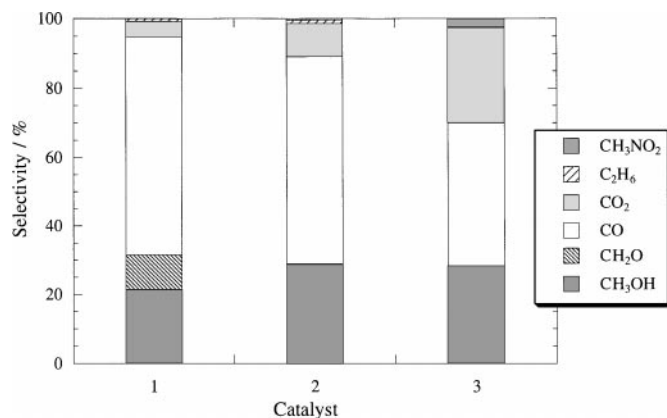

FIG. 2. Variation of product selectivity with reaction time using a Cu–ZnO/Al$_2$O$_3$ catalyst. Catalyst: sample A. Catalyst weight: 0.5 g. Flow rate, reaction pressure, reaction temperature, catalyst bed temperature, and feed gas composition are as in Fig. 1.

conversions were almost the same (5.3–5.5%) as shown in the figure caption. The products in the reactions of CH$_4$–O$_2$–NO in the absence of catalyst were CH$_3$OH, CH$_2$O, CO, and a few CO$_2$ and C$_2$H$_6$. The selectivities of products clearly changed from the absence to the presence of Cu–ZnO/Al$_2$O$_3$ catalyst. The selectivities of CH$_3$OH and CO$_2$ increased and those of CH$_2$O and CO decreased in the presence of both samples A and B. CH$_2$O was hardly detected in the presence of these catalysts. Only CH$_3$OH was observed as the oxygenate in the products in the presence of Cu–ZnO/Al$_2$O$_3$. The selectivity of CH$_3$OH in the presence of sample A was almost the same as that of sample B. The selectivities of CO$_2$ and CH$_3$NO$_2$ increased more in the presence of sample B than sample A.

Figure 2 shows the variation of selectivity as a function of the time course of the direct selective oxidation of CH$_4$ in the presence of sample A. The reaction conditions were the same as those described in Fig. 1. All CH$_4$ conversion values through the reaction from 20 min to 300 min were almost the same (5.4–5.6%). The selectivities of products clearly changed with reaction time, and almost stabilized after 180 min. CO$_2$ was the main product at 20 min; thereafter the selectivities of CO and CH$_3$OH increased until 180 min. CH$_2$O was hardly observed through the reaction. These variations of selectivities in the course of reaction time were not observed in the absence of catalyst.

Figure 3 shows the effects of catalyst weight variations with sample A on the selectivities of the products. All of the reaction conditions were the same as described in Figs. 1 and 2. CH$_4$ conversion at 550°C in the absence of catalyst was 5.5 %. All CH$_4$ conversion values in the presence of sample A were included in the region 5.3–5.6%. Product selectivity was measured after reaction for 180 min. The selectivity of CH$_3$OH increased up to 0.5 g, then slightly decreased. The selectivity of CH$_2$O disappeared in the presence of more than 0.1 g of sample A catalyst.

FIG. 1. Effects of catalysts on product selectivities. Catalyst: (1) in the absence of catalysts, (2) in the presence of sample A, (3) in the presence of sample B. Catalyst weight: 0.5 g. Flow rate: 120 ml min^{-1}. Reaction pressure: 0.5MPa. Gas-phase reaction temperature: 550°C. Catalyst bed temperature: 250°C. Feed gas composition: 77.5%, CH$_4$; 5.8%, O$_2$; 0.5%, NO; 16.2%, Ar, respectively. CH$_4$ conversion: (1) 5.5%, (2) 5.4%, (3) 5.4%. Each selectivity was measured after reaction for 180 min.
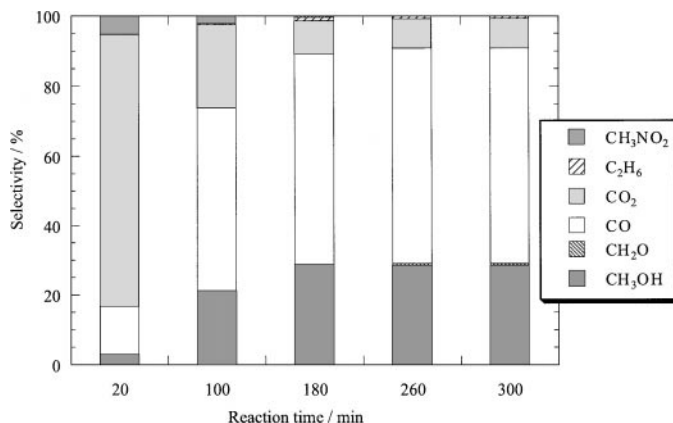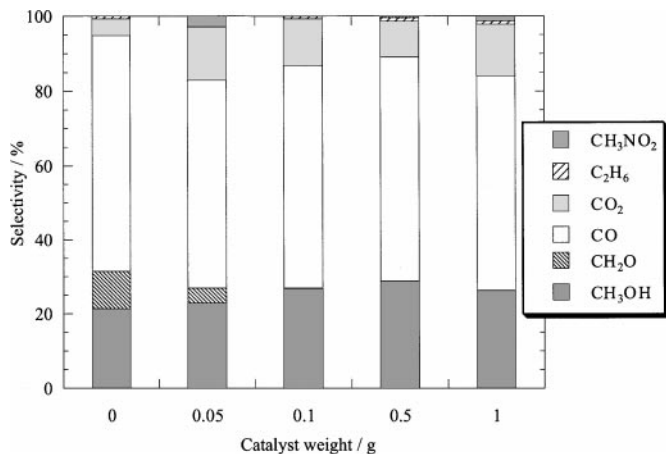
FIG. 3.   Effects of catalyst weight on product selectivity. Catalyst: sample A. Reaction time: 180 min except for the catalyst weighting 1.0 g (380 min). Flow rate, reaction pressure, reaction temperature, catalyst bed temperature, and feed gas composition are as in Fig. 1.

The conversion and selectivity of gas-phase reaction temperatures at both 500 and 550°C in the presence and absence of catalysts are listed in Table 1. Every test in the presence of catalyst was examined with sample A. Catalyst temperature was stabilized at 250°C in every test. The selectivity of every product was measured after reaction for 180 min. The selectivities of CH_3OH in the absence of catalyst were almost the same at 500 and 550°C. The CH_2O produced was partly oxidized to CO at 550°C in the absence of catalyst. In marked contrast to these variations between 500 and 550°C in the absence of catalyst, CH_3OH, CH_2O, and CO were almost oxidized to CO_2 at 500°C in the presence of sample A catalyst. The selectivities of CH_3OH and CO were raised at 550°C in comparison with those at 500°C in the presence of $Cu–ZnO/Al_2O_3$; however, the selectivity of CH_2O was still low at 550°C in the presence of catalyst. Moreover, the selectivity of CH_3OH in the presence of catalyst exceeded that at 550°C in the absence of catalyst. The selectivity of CO at 550°C in the presence of catalyst was close to that at 550°C in the absence of catalyst. The selectivity of CO_2 was quite smaller than that at 500°C in the presence of catalyst.
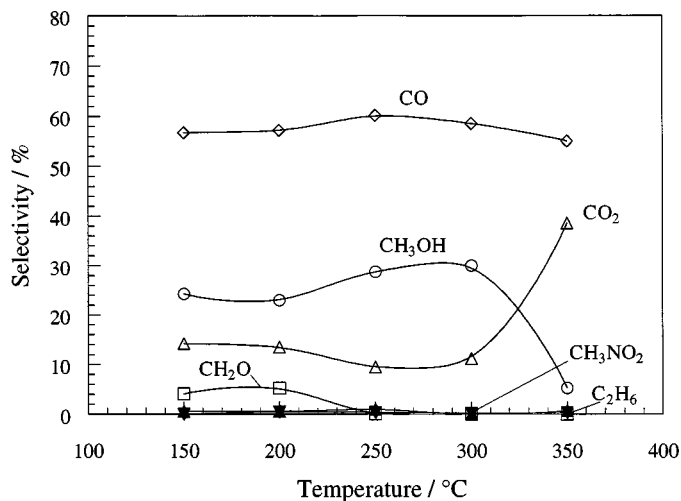

FIG. 4.   Effects of catalyst bed temperature on product selectivity. Catalyst: sample A. Catalyst weight 0.5 g. Flow rate, reaction pressure, reaction temperature, reaction time, and feed gas composition are as in Fig. 1.

These differences between 500 and 550°C were assumed to be brought about by the differences of amount of remaining oxygen over the catalysts. The conversions of O_2 at 500 and 550°C in the presence of sample A were 85.8 and 99.5%, respectively. Oxygen in the feed gas was almost used up at 550°C in the gas-phase selective oxidation of CH_4. Taylor *et al.* (18) reported that CO was oxidized to CO_2 in the presence of O_2 over Cu–ZnO catalyst. We assumed that CH_3OH, CH_2O, and CO were oxidized to CO_2 at 500°C over $Cu–ZnO/Al_2O_3$ catalyst with oxygen.

Figure 4 shows the effects of catalyst temperatures on the selectivities of products in the reaction of $CH_4–O_2–NO$ with sample A. The temperature of the gas-phase selective oxidation of CH_4 was 550°C in every test. All CH_4 conversion values through the variation of catalyst temperature were almost the same (5.4–5.7%). CH_2O was observed at temperatures lower than 250°C in the presence of catalyst. The selectivity of CH_3OH increased up to 300°C, then rapidly decreased above 300°C. The selectivity

TABLE 1

Effects of the Gas-Phase Reaction Temperature in the Absence and Presence of Cu–ZnO-Based Catalysts

No.	Temp. (°C)	Catalyst (g)	Conversion (%)		Selectivity (%)						
			CH_4	O_2	CH_3OH	CH_2O	CO	CO_2	C_2H_4	C_2H_6	CH_3NO_2
1	500	0[a]	3	57.2	21	17.8	48	6.9	0	0.3	6
2	500	0.5	3.3	85.8	0	0.4	0.1	99.5	0	0	0
3	550	0[a]	5.5	99	21.4	10.1	63.3	4.4	0	0.8	0
4	550	0.5	5.4	99.5	28.8	0.1	60.2	9.5	0	1	0.4

Note. Catalyst: sample A, flow rate: 120 ml min^{-1}, reaction pressure: 0.5 MPa, reaction time: 180 min, catalyst bed temperature: 250°C; feed gas composition: 77.5% CH_4, 5.8% O_2, 0.5% NO, 16.2% Ar.
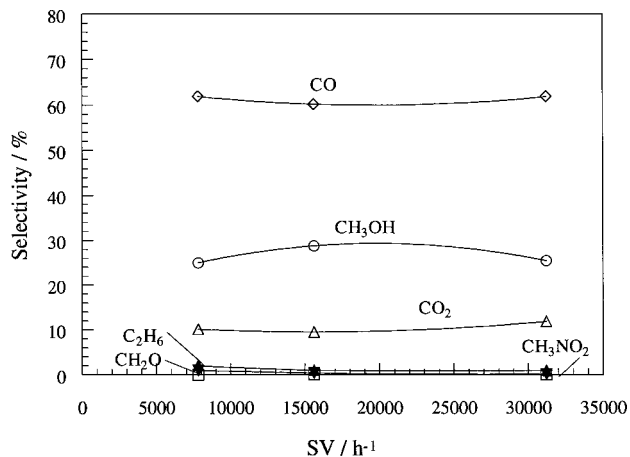   [a] In the absence of the catalyst.

FIG. 5. Effects of space velocity on product selectivity. Catalyst: sample A. Catalyst weight: 0.5 g. Flow rates were 60 ml min^{-1} (SV = 7800 h^{-1}), 120 ml min^{-1} (SV = 15,600 h^{-1}), and 240 ml min^{-1} (SV = 31,200 h^{-1}). Reaction pressure, reaction temperature, catalyst bed temperature, reaction time, and feed gas composition are as in Fig. 1.

FIG. 6. Effects of ratio of CH_4 to O_2 in the feed gas on product selectivity. Catalyst: sample A. Catalyst weight: 0.5 g. Flow rate, reaction pressure, reaction temperature, catalyst bed temperature, and reaction time are as in Fig. 1.

of CO varied slightly through the change in temperature of Cu–ZnO/Al$_2$O$_3$ from 150 to 350°C. The selectivity of CO$_2$ increased rapidly above 300°C, in marked contrast to the decrease in selectivity of CH$_3$OH. Breen *et al.* (19) reported that the reactivities of the steam reforming of methanol over Cu–ZnO/ZrO$_2$/Al$_2$O$_3$ were increased above around 350°C. We assumed that the steam reforming reaction between the CH$_3$OH and H$_2$O produced over Cu–ZnO/Al$_2$O$_3$ progressed from around 350°C:
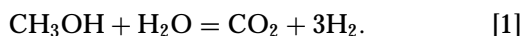
$$CH_3OH + H_2O = CO_2 + 3H_2. \qquad [1]$$

Figure 5 shows the effects of SV variation on the selectivities of products in the presence of sample A. All CH$_4$ conversion values through the variation in SV were in the region 5.3–5.6%. Through the variation of SV from 7800 h^{-1} (60 ml min^{-1}) to 31,200 h^{-1} (240 ml min^{-1}) at 550°C, the selectivity of every product, i.e., CH$_3$OH, CO, CO$_2$, and others, hardly changed.

Figure 6 shows the effects of CH$_4$/O$_2$ ratio on the selectivities of products in the presence of sample A. Conversion of CH$_4$ is also shown in the figure. The temperature of the gas-phase reaction of CH$_4$ was stabilized at 550°C in every test. Catalyst temperature was 250°C in every test. CH$_4$ conversion decreased monotonously with decreasing proportion of oxygen. The selectivity of CO slightly decreased and those of CH$_3$OH and CO$_2$ slightly increased in the region of a higher proportion of CH$_4$.

DISCUSSION

First, we measured the amount of hydrogen produced with the same gas chromatographs to determine the reaction path of formation of CH$_3$OH over Cu–ZnO/Al$_2$O$_3$
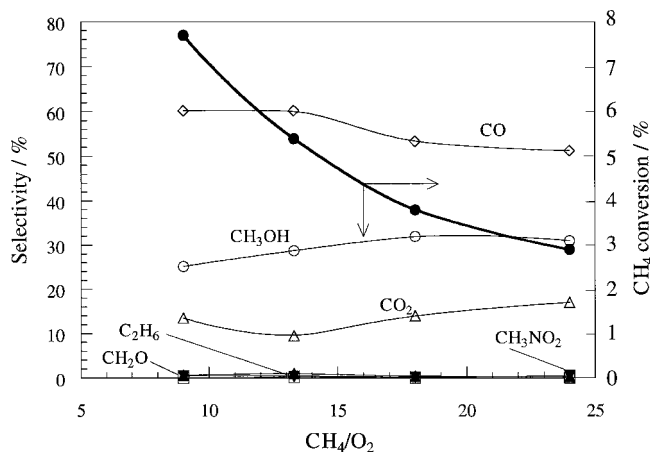
catalyst. Therefore, we lowered the temperature of the column for TCD from 90 to 60°C. Reaction conditions were the same as in Fig. 1. The ratio of volume of hydrogen produced to that of methane reacted was 0.32 in the absence of catalyst. That ratio in the presence of sample A was 0.39. The temperature of the catalyst was 250°C.

Second, we calculated the thermodynamic equilibrium values of products using the CHEMKIN III program so as to discuss the reaction paths over Cu–ZnO/Al$_2$O$_3$ (Table 2). The initial molar proportion of simulation gas in Run 1 in the table was almost the same as the experimentally observed one, i.e., CO 0.01, H$_2$ 0.03, inert gas 0.96. The expected selectivity of methanol, which was calculated from the equilibrium values predicted for methanol, CO, CO$_2$, and CH$_2$O as given in the table footnote, was 0.0046%. The expected selectivity of methanol from CO$_2$ and H$_2$ under the same reaction conditions was 0.0007%. The production of methanol from CO/H$_2$ or CO$_2$/H$_2$ under these reaction conditions could not be expected. In

TABLE 2

Thermodynamic Simulation of the Equilibrium Methanol Formation

Run	Pressure (MPa)	Temp. (°C)	Initial state (%)					Equilibrium CH$_3$OH formation[a] (%)
			CO	CO$_2$	H$_2$	CH$_2$O	inert gas	
1	0.5	250	1	—	3	—	96	0.00462
2	0.5	250	—	1	3	—	96	0.000672
3	0.5	250	—	—	1.2	0.4	98.4	99.0
4	0.1	250	—	—	1.2	0.4	98.4	95.1

Note. Used simulation software: CHEMKIN III EQUIP application software.

[a] Equibrium CH$_3$OH formation (%) = 100 × [CH$_3$OH]$_{eq.}$/[CO + CO$_2$ + CH$_2$O + CH$_3$OH]$_{eq.}$.

contrast to these results, the predicted selectivity of methanol produced through the reaction between CH_2O and H_2 was 99.0% under reaction conditions close to those described in Fig. 1. This predicted selectivity of methanol produced via CH_2O was 95.1% even when the reaction pressure was 0.1 MPa (Table 2). We experimentally checked the reactions of CO/H_2 and CO_2/H_2 in the same reactor with the $Cu–ZnO/Al_2O_3$ catalyst (sample A). The feed gas composition was 1% CO or 1% CO_2 and 3% H_2 with Ar as a balanced gas. The temperatures of the gas-phase reaction of CH_4 and catalyst and reaction pressure were the same as those in Fig. 1. Production of CH_3OH was not detected with gas chromatographs in the reactions of both CO/H_2 and CO_2/H_2 with sample A catalyst.

We experimentally examined the reactivities of $Cu–ZnO/Al_2O_3$ catalysts in the hydrogenation of CH_2O (Fig. 7). The procedures were described under Experimental. Reaction pressure was 0.1 MPa. CH_2O conversion increased with catalyst temperature, and reached 100% in the region from 150 to 200°C with the $Cu–ZnO/Al_2O_3$ catalysts. The selectivity of the CH_3OH produced fell quickly above 150°C. The selectivity of CH_3OH in the products was close to 0% at 200°C with the sample A catalyst. CO_2 (95.6%) and CO (1.8%) were observed at 200°C in the products. Other products were not observed at 200°C, however; methyl formate

and formic acid were detected at reaction temperatures lower than 200°C. We therefore considered the reaction pathways over the sample A catalyst at 200°C as

$$CH_2O + H_2 = CH_3OH \qquad [2]$$

and Eq. [1]: $CH_3OH + H_2O = CO_2 + 3H_2$. H_2O was included in the feed gas (12.7%). With respect to the small selectivity of CO at 200°C in the products, a few CH_2O might be dissociated over the catalyst:

$$CH_2O = CO + H_2. \qquad [3]$$
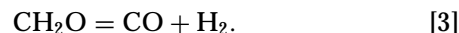
We examined the effects of temperature of $Cu–ZnO/Al_2O_3$ catalyst on the selectivity of products (Fig. 4). The selectivity of CH_2O decreased above 200°C but that of CH_3OH reached the maximum at 300°C in Fig. 4. However, the selectivity of CH_3OH decreased quickly above 150°C in Fig. 7. The temperature difference at maximum CH_3OH selectivity in Figs. 4 and 7 could be a result of the difference in reaction conditions, especially the amount of H_2O in the reactant gas.

From the calculated values of thermodynamic equilibrium of CH_3OH produced in the reactant gases of CO/H_2, CO_2/H_2, and CH_2O/H_2, we assumed the CH_3OH produced over $Cu–ZnO/Al_2O_3$ catalyst in the reactions of $CH_4–O_2–$ NO was produced in the reaction of Eq. [2]. The experimental results of the reactions in the reactant gases CO/H_2, CO_2/H_2, and CH_2O/H_2 also suggested that the pathway of formation of CH_3OH in the reaction of $CH_4–O_2–NO$ in the presence of $Cu–ZnO/Al_2O_3$ catalyst was CH_2O hydrogenation.

With respect to the variation of selectivity in the time course of the reaction of $CH_4–O_2–NO$ in the presence of $Cu–ZnO/Al_2O_3$ catalyst in Fig. 2, we considered that O_2 in the reactant gas was gradually consumed through the progress of the gas-phase selective oxidation of methane. $Cu–ZnO/Al_2O_3$ catalysts therefore were gradually reduced with the decreases in the amount of O_2 in the reactant gas, then catalyzed the formation of CH_3OH in Eq. [2]. Kakumoto and Watanabe (20) reported that methanol synthesis from CO_2 and H_2 over a $Cu–ZnO$ catalyst proceeded on the Cu(I) site of the catalyst through formate and formaldehyde intermediates from their theoretical calculation with the ab initio methods. Therefore the variation of $Cu–ZnO/Al_2O_3$ catalyst, especially the copper state, accompanied by the variation of O_2 concentration in the reactant gas brought about the variation of selectivity in the time course of the reaction of $CH_4–O_2–NO$ in the presence of $Cu–ZnO/Al_2O_3$ catalyst in Fig. 2.

We ensured the presence of H_2 in the products of the reaction of $CH_4–O_2–NO$ in both the absence and presence of $Cu–ZnO/Al_2O_3$ catalyst as mentioned above. It was ensured that the hydrogen and CH_2O in the products reacted to produce CH_3OH over $Cu–ZnO/Al_2O_3$ catalyst.
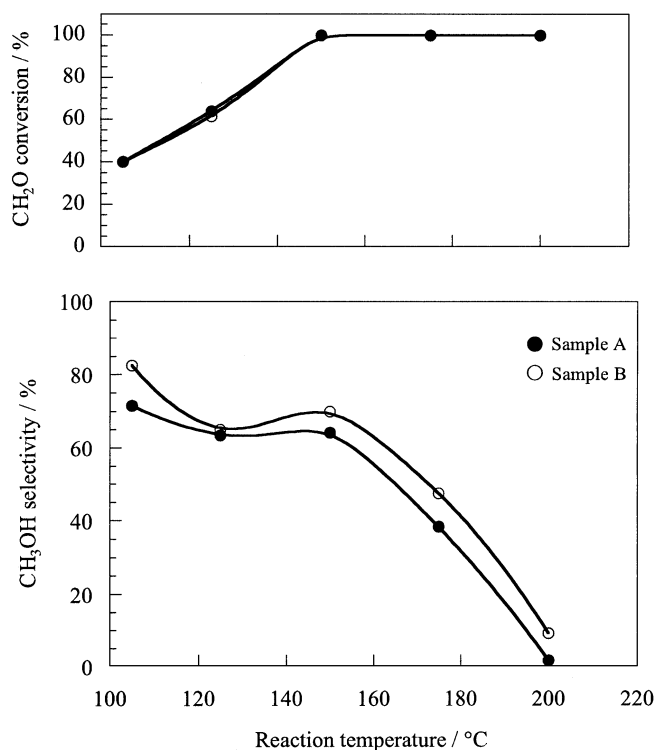

FIG. 7. CH_2O conversion and CH_3OH selectivity as functions of reaction temperature. Catalyst: sample A. Catalyst weight: 1.0 g. Flow rate: 70 ml/min. Reaction pressure: 0.1 MPa. Feed gas composition: CH_2O: 5.0% H_2: 38.6%; CH_3OH: 0.9%; H_2O: 12.7%; Ar: balance.

Moreover, the ratio of H_2 produced to CH_4 reacted increased (0.32–0.39) in the presence of Cu–ZnO/Al$_2$O$_3$ catalyst in the reaction of CH_4–O_2–NO. The selectivity of CO decreased and that of CO_2 increased with the Cu–ZnO/Al$_2$O$_3$ catalyst in comparison to the absence of the catalyst as shown in Table 1 (gas-phase reaction temperature: 550°C; Cu–ZnO/Al$_2$O$_3$ catalyst temperature: 250°C). We suspected the coexistence of the water–gas shift reaction (12),

$$CO + H_2O = CO_2 + H_2, \qquad [4]$$
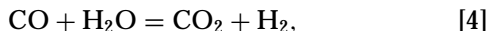
over the Cu–ZnO/Al$_2$O$_3$ catalyst (sample A) in the reaction of CH_4–O_2–NO.

We experimentally examined the reactivity of Cu–ZnO/Al$_2$O$_3$ catalyst in the WGSR using the same reactor as in the reaction of CH_4–O_2–NO. Reaction pressure was 0.5 MPa. The temperature of the sample A catalyst was 250°C. Percentages of CO (6.4%) and H_2O (42.6%) in the feed gas decreased to 0.6 and 36.8%, respectively, through the WGSR in the presence of sample A catalyst. The products of WGSR, CO_2 and H_2, increased in comparison to those in the feed gas, respectively (CO_2: 8.2 → 14.0%; H_2 41.2 → 47.0%). Therefore we ensured that the WGSR and the formation of CH_3OH in Eq. [2] progressed simultaneously over the Cu–ZnO/Al$_2$O$_3$ catalyst at 250°C in the reaction of CH_4–O_2–NO.

We suggested two reactions, i.e., Eqs. [2] and [4], over Cu–ZnO/Al$_2$O$_3$ catalyst at 250°C as the catalyst temperature. The selectivity of CH_3OH was almost the same with sample A and sample B (Fig. 1). However, the selectivities of CO and CO_2 were clearly different as shown in the figure. The selectivity of CO decreased and that of CO_2 increased with the sample B catalyst at 250°C. It was assumed that the water–gas shift reaction progressed more over sample B catalyst. The XRD spectra of these samples were almost the same. We assumed the differences in Cu/Zn atomic ratio measured with XPS on the surface of the catalyst (sample A: 0.88, sample B: 0.65) and/or specific surface area (sample A: 68.7 m^2/g, sample B: 93.1 m^2/g) brought about the difference in selectivities of CO and CO_2 in the products (Fig. 1). The lower surface ratio of Cu/Zn and/or higher specific surface area could be effective in promoting the WGSR over Cu–ZnO/Al$_2$O$_3$ catalyst. However, the formation of CH_3OH was not affected by these differences.

CONCLUSIONS

Three distinct reaction paths over Cu–ZnO/Al$_2$O$_3$ catalyst were detected in the gas-phase selective oxidation of methane in CH_4–O_2–NO. The formation of CH_3OH from CH_2O–H_2 and the water–gas shift reaction of CO–H_2O progressed at around 250°C over Cu–ZnO/Al$_2$O$_3$ catalyst. The steam reforming reaction of CH_3OH also progressed

over Cu–ZnO/Al$_2$O$_3$ catalyst at around 350°C and above. Both CH_3OH and CH_2O were observed as C$_1$-oxygenates at 550°C in the gas-phase selective oxidation of CH_4 in CH_4–O_2–NO without Cu–ZnO/Al$_2$O$_3$ catalyst, but then only CH_3OH was observed in the presence of Cu–ZnO/Al$_2$O$_3$ catalyst in addition to the direct gas-phase selective oxidation of methane. Catalyst temperature was 250°C and reaction pressure was 0.5 MPa. Although the selectivity of CH_3OH was almost the same, the selectivity of CO decreased and that of CO_2 increased in the products of the reaction of CH_4–O_2–NO in the presence of catalyst with a lower surface Cu/Zn atomic ratio and a higher specific surface area.

REFERENCES

1. Newitt, D. M., and Huffner, A. E., *Proc. R. Soc. London, A Math. Phys. Sci.* **147**, 555 (1934).
2. Arutyunov, V. S., Basevich, V. Y., and Vedeneev, V. I., *Russ. Chem. Rev.* **65**, 197 (1996).
3. Pitchai, R., and Klier, K., *Catal. Rev. Sci. Eng.* **28**, 13 (1986).
4. Gesser, H. D., Hunter, N. R., and Prakash, C. B., *Chem. Rev.* **85**, 235 (1985).
5. Irusta, S., Lombardo, E. A., and Miro, E. E., *Catal. Lett.* **29**, 339 (1994).
6. Han, L. B., Tsubota, S., and Haruta, M., *Chem. Lett.*, 931 (1995).
7. Otsuka, K., Takahashi, R., Amakawa, K., and Yamanaka, I., *Catal. Today* **45**, 23 (1998).
8. Otsuka, K., Takahashi, R., and Yamanaka, I., *J. Catal.* **185**, 182 (1999).
9. Bañares, M. A., Cardoso, J. H., Hutchings, G. J., Bueno, J. M. C., and Fierro, J. L. G., *Catal. Lett.* **56**, 149 (1998).
10. Teng, Y., Tabata, K., Sakurai, H., and Suzuki, E., *Appl. Catal. A* **190**, 283 (2000).
11. Tabata, K., Teng, Y., Yamaguchi, Y., Sakurai, H., and Suzuki, E., *J. Phys. Chem. A* **104**, 2648 (2000).
12. Rhodes, C., Hutchings, G. J., and Ward, A. M., *Catal. Today* **23**, 43 (1995).
13. Klier, K., *Adv. Catal.* **31**, 243 (1982).
14. Wainwright, M. S., and Trimm, D. L., *Catal. Today* **23**, 29 (1995).
15. Kee, R. J., Rupley, F. M., and Meek, E., CHEMKIN-III: A Fortran Chemical Kinetic Package for the Analysis of Gas Phase Chemical and Plasma Kinetics, Report SAND 96-8216, Sandia National Laboratories, Livermore, CA, 1996.
16. Lutz, A. E., Kee, R. J., and Miller, J. A., SENKIN: A Fortran Program for Predicting Homogeneous Gas Phase Chemical Kinetics with Sensitivity Analysis, Report SAND 87-8248, Sandia National Laboratories, Livermore, CA, 1988.
17. Kee, R. J., Rupley, F. M., and Miller, J. A., The CHEMKIN Thermodynamic Data Base, Report SAND 87-8215B, Sandia National Laboratories, Livermore, CA, 1990.
18. Taylor, S. H., Hutchings, G. J., and Mirzaei, A. A., *Chem. Commun.*, 1373 (1999).
19. Breen, J. P., Meunier, F. C., and Ross, J. R. H., *Chem. Commun.*, 2247 (1999).
20. Kakumoto, T., and Watanabe, T., *Catal. Today* **36**, 39 (1997).